

Hybrid Heat Pump Flexibility Allocation: Quantified Thermal Comfort-Based Congestion Management

Abstract—Congestion management has garnered significant attention in the Netherlands due to the sharply rising pressure on the limited capacity of distribution networks. As an increasingly deployed flexible asset, hybrid heat pumps can help mitigate congestion in distribution networks. However, one key challenge in allocating flexibility during congestion management is to ensure user thermal comfort. In this context, this work proposes the incorporation of quantified thermal comfort into the modeling of congestion management using hybrid heat pumps. The grid topology model is constructed based on a field-collected low-voltage distribution network in the Netherlands, where end-user thermal comfort is quantified based on a real dataset, and integrated into the optimization objective of the congestion management model. The methodology is tested on a practical case study in the Netherlands, where flexibility allocation under different power limitation levels is analyzed. The results demonstrate how flexibility allocation and pricing change under varying congestion management requirements and their impact on user thermal comfort.

Index Terms—Congestion management, Flexibility, Hybrid heat pump, Thermal comfort, Distribution network

I. INTRODUCTION

With the rapid expansion in distributed renewable energy, grid congestion has emerged as a significant challenge in distribution networks, particularly in the Netherlands [1]. Therefore, congestion management has attracted considerable attention [2]. At the same time, system operators are investigating strategies to ensure the availability of more flexible capacity in congested grids, by for example mandating flexibility provision from large consumers [3].

The Dutch residential sector is seeing rapid growth in hybrid heat pump (HHP) adoption [4], with their inherent gas-electricity flexibility making them a scalable flexibility resource to alleviate peak load in low-voltage grids. The current literature has demonstrated the effective performance of HHPs in providing flexibility when needed [5]. In the practical control of HHPs for flexibility provisioning, researchers have taken into consideration numerous factors, such as energy cost [6], carbon reduction [7], and user comfort [8]. Among these factors, thermal comfort has garnered the most attention, although it remains challenging to quantify [9].

Consequently, researchers have proposed various approaches to address the quantification challenges [10]. Usually, hierarchy and dynamism metrics would be proposed to evaluate occupants' feeling [11] which are too complex

to apply in practical cases. With the objective to reduce the complexity, [12] measured thermal comfort using interior temperature which can not directly capture human perception. To address this limitation, some scholars have introduced the Predicted Mean Vote (PMV) index [13], albeit primarily at the assessment stage rather than during optimization and control [14] due to its complex formulation. Xu *et al.* [15] investigated methods to simplify the PMV and incorporate it into an optimization framework. However, their approach only employs a simplified linear function for thermal comfort with theoretically derived parameters. Overall, methods for quantifying thermal comfort are neither aligned with real-world scenarios nor can they be readily integrated into the congestion management optimization framework.

To address the research gap mentioned above, this work quantifies thermal comfort using parameters validated through pilot implementations and proposes a thermal comfort-based congestion management method within a real-world project. In addition to the inclusion of energy costs in congestion management [16], this study also accounts for costs associated with participant comfort, describing the price acceptance rate of potential consumers. Specifically, it first introduces a real-life operational data-driven thermal comfort model. Next, both energy and thermal comfort costs are integrated into the optimization framework of congestion management. Finally, it provides a detailed discussion of various flexibility allocation strategies, their corresponding flexibility prices, and the thermal comfort of the participants during flexibility provision.

This research is conducted as part of the DACS-HW project [17], which investigates how HHPs can participate in congestion management. DACS-HW facilitates collection of operational data of HHPs, electrical consumption data of participant smart meters and low-voltage distribution grid transformer data, such as phase voltages and currents.

The remainder of the paper is organized into four sections. Section II explains the developed methodology. Section III presents the case study's setup, which describes the input data characteristics and discusses the obtained results, while Section IV concludes the paper.

II. PROPOSED METHODOLOGY

As shown in Fig. 1, the proposed methodology can be described in five stages: i) low-voltage distribution network modeling using real network data, ii) HHP and thermal dynamic modeling, thereby enabling the modeling of the entire grid operation, iii) thermal comfort quantification, linearization, incorporation in the objective function, iv) simulation of

This work is part of the DACS-HW project (MOOI322001) which received funding from the Topsector Energie MOOI subsidy program of the Netherlands Ministry of Economic Affairs and Climate Policy, executed by the Netherlands Enterprise Agency (RVO).

TABLE I
NOMENCLATURE

| Sets | |
|--|---|
| \mathcal{B} | Buses $i \in \mathcal{B}$ in the network, $i = 0$ is the slack bus. |
| $\mathcal{H} \subseteq \mathcal{B}$ | Subset of buses connected to a user. |
| $\mathcal{H}^H \subseteq \mathcal{H}$ | Subset of user buses that have a HHP. |
| \mathcal{L} | Set of lines $i \rightarrow j$ in the network with $(i, j) \in \mathcal{L}$. |
| \mathcal{T} | Set of discrete time periods with interval Δt . |
| Parameters | |
| Δt | Time interval [hours]. |
| λ_t^p | Electricity price [€/kWh]. |
| λ_t^g | Natural gas price [€/m ³]. |
| λ_{comf} | Thermal comfort price [€/%]. |
| η_g, H_g | Efficiency of boiler, heating value of gas: 9.77 [kWh/m ³] |
| S_0^{max} | Maximum transformer apparent power [kVA]. |
| \underline{V}, \bar{V} | Voltage magnitude safety constraints [V]. |
| $p_i^{\text{base}}, q_i^{\text{base}}$ | Fixed real and reactive base load at bus i [kW, kVar]. |
| Variables | |
| $s_i = s_i^g - s_i^d$ | Net apparent power injection at bus i . |
| $p_i = p_i^g - p_i^d$ | Net real power injection at bus i . |
| $q_i = q_i^g - q_i^d$ | Net reactive power injection at bus i . |
| S_{ij}, Q_{ij}, P_{ij} | Apparent, reactive, real power sent from bus i to bus j . |
| v_i | Squared voltage magnitude $ V_i ^2$ at bus i . |
| l_{ij} | Squared current magnitude $ I_{ij} ^2$ from bus i to j [A ²]. |
| $g_{i,t}$ | Gas consumed at bus i time t [m ³]. |
| p_i^{HP} | Heat pump electrical power consumption at bus i [kW]. |
| η_{COP} | Coefficient of Performance (COP) of heat pump in HHP. |
| T^i, T^h, T^a | Interior, emission, house envelope temperature [°C]. |
| $\Phi_{i,t}^{\text{CV}}, \Phi_{i,t}^{\text{HP}}, \Phi_{i,t}^h$ | Boiler, heat pump, combined thermal power in [kW]. |
| $z_{i,t}^{\text{HP}}, z_{i,t}^{\text{CV}}$ | Whether to supply heat with heat pump or boiler. |
| p_t^{imp} | Imported electrical power [kW]. |

the baseline case based the historical data and proposed model, v) congestion management results based on different power limitation levels. The notation used in this paper is defined in Table I.

A. Distribution Network Model

To model the non-convex and nonlinear Optimal Power Flow (OPF) in the low-voltage distribution network, the Second-Order Cone Programming (SOCP) approach is employed to relax the problem, while also accounting for grid losses to improve the accuracy of the results [18].

The electrical grid model is defined by imposing feasibility constraints on the power flows and currents between buses, and the voltages at bus terminals. The equations summarized below are adopted from the conic relaxation of the branch flow

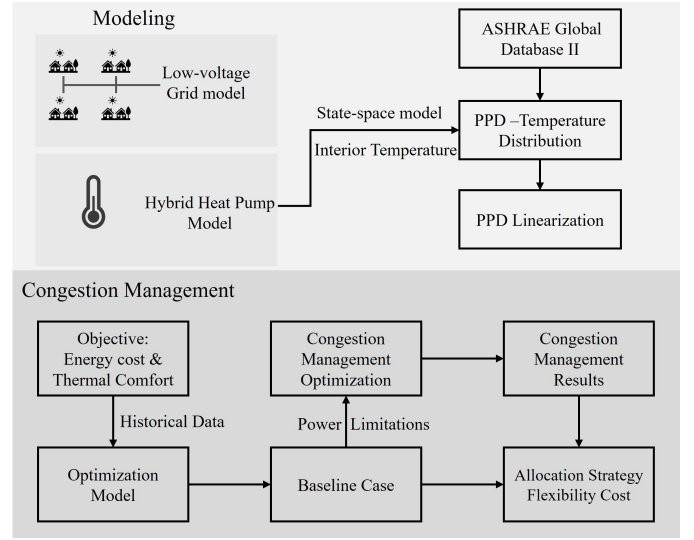


Fig. 1. Overview of the Proposed Method

model [19].

$$p_j = \sum_{(j,k) \in \mathcal{L}} P_{jk} - \sum_{(i,j) \in \mathcal{L}} (P_{ij} - r_{ij} l_{ij}) \quad \forall j \in \mathcal{B} \quad (1a)$$

$$q_j = \sum_{(j,k) \in \mathcal{L}} Q_{jk} - \sum_{(i,j) \in \mathcal{L}} (Q_{ij} - x_{ij} l_{ij}) \quad \forall j \in \mathcal{B} \quad (1b)$$

$$v_j = v_i - 2(P_{ij} r_{ij} + Q_{ij} x_{ij}) \quad \forall (i, j) \in \mathcal{L} \quad (1c)$$

$$+ (r_{ij}^2 + x_{ij}^2) l_{ij}$$

$$l_{ij} \geq \frac{P_{ij}^2 + Q_{ij}^2}{v_i} \quad \forall (i, j) \in \mathcal{L} \quad (1d)$$

The following operational constraints are imposed on the control variables:

$$P_0^2 + Q_0^2 \leq (S_0^{\text{max}})^2 \quad (2a)$$

$$l_{ij} \leq \bar{l}_{ij} \quad \forall (i, j) \in \mathcal{L} \quad (2b)$$

$$\underline{V} \leq v_i \leq \bar{V} \quad \forall i \in \mathcal{B} \quad (2c)$$

Furthermore, we assume no generators are present at any of the user buses and all power supplied to the network S_0 is transferred through the slack bus, which is connected to the grid transformer. This results in the following simplified load conditions:

$$p_i = 0 \quad \forall i \in \mathcal{B} \setminus \{\mathcal{H}, \{0\}\} \quad (3a)$$

$$p_i = -p_i^{\text{base}} \quad \forall i \in \mathcal{H} \setminus \mathcal{H}^H \quad (3b)$$

$$p_i = -p_i^{\text{base}} - p_i^{\text{HP}} \quad \forall i \in \mathcal{H}^H \quad (3c)$$

$$q_i = -q_i^{\text{base}} - q_i^{\text{HP}} \quad \forall i \in \mathcal{H}^H \quad (3d)$$

$$q_i^{\text{HP}} = \tan(\arccos(\text{PF})) \cdot p_i^{\text{HP}} \quad \forall i \in \mathcal{H}^H \quad (3e)$$

Based on real operational performance, under continuous load conditions heat pumps typically behaves as an inductive load with a power factor of $\text{PF} \approx 0.9$, this relationship is modelled by (3e).

B. Hybrid Heat Pump Model

The HHP of each household is driven by the thermal dynamics described by the discrete state-space model (4a), of which the state-space matrices have been identified from DACS-HW field data [17]. A more detailed description of the thermal model deployed here and a theoretical background can be found in [20]. Constraint (4b) sets the initial condition for the temperature state trajectory.

$$\mathbf{T}_{i,t+1} = \mathbf{A}\mathbf{T}_{i,t} + \mathbf{B}\mathbf{u}_{i,t} \quad \forall t \in \mathcal{T}, \forall i \in \mathcal{H}^H \quad (4a)$$

$$\mathbf{T}_{i,1} = \mathbf{T}^{\text{init}} \quad \forall i \in \mathcal{H}^H \quad (4b)$$

The supply water temperature and emission system temperature T_h are closely related quantities and assumed here to be approximately equal. The COP model η_{COP} is a nonlinear function of the temperature lift $T^h - T^a$, preventing it from being directly used in a linear optimization model. The common and most simple approach to deal with the nonlinearity is fixing T_h to an operating point $T_h = T_h^0$ [21–23]. This operating point can be derived from operational data, but depends significantly on various environmental factors such as the installation quality, the type of emission system, and the heat demand required.

The regression coefficients of η_{COP} were found through linear regression by fitting on the DACS-HW dataset [17]. The electrical consumption of a HHP, P^{HP} , is determined by the COP, and hence also depends on T_h . This makes the choice of T_h^0 a critical parameter in the simulation, and ideally a range of supply temperatures should be simulated to understand the consequences of supply temperature on electrical grid loading. The COP model is defined by the following equations:

$$\eta_{\text{COP}}(\Delta T) = 20.3795 - 3.2103 \log_2(1 + \Delta T) \quad (5a)$$

$$T_{i,t}^h - T_t^a = \Delta T_{i,t} \quad \forall t \in \mathcal{T}, \forall i \in \mathcal{H}^H \quad (5b)$$

$$\Phi_{i,t}^{\text{HP}} = \eta_{\text{COP}}(\Delta T_{i,t}) \cdot P_{\text{max}}^{\text{HP}} \quad \forall t \in \mathcal{T}, \forall i \in \mathcal{H}^H \quad (5c)$$

The inputs of the HHPs are limited to the feasible set given by constraints (6a) - (6e), which is derived from real operational data.

$$z_{i,t}^{\text{CV}} \Phi_{\text{min}}^{\text{CV}} \leq \Phi_{i,t}^{\text{CV}} \leq z_{i,t}^{\text{CV}} \Phi_{\text{max}}^{\text{CV}} \quad \forall t \in \mathcal{T}, \forall i \in \mathcal{H}^H \quad (6a)$$

$$z_{i,t}^{\text{HP}} \Phi_{\text{min}}^{\text{HP}} \leq \Phi_{i,t}^{\text{HP}} \leq z_{i,t}^{\text{HP}} \Phi_{\text{max}}^{\text{HP}} \quad \forall t \in \mathcal{T}, \forall i \in \mathcal{H}^H \quad (6b)$$

$$0 \leq P_{i,t}^{\text{HP}} \leq P_{\text{max}}^{\text{HP}} \quad \forall t \in \mathcal{T}, \forall i \in \mathcal{H}^H \quad (6c)$$

$$\Phi_{i,t}^{\text{CV}} + \Phi_{i,t}^{\text{HP}} = \Phi_{i,t}^h \quad \forall t \in \mathcal{T}, \forall i \in \mathcal{H}^H \quad (6d)$$

$$(1/\Delta t) \cdot g_{i,t} \eta^g H^g = \Phi_{i,t}^{\text{CV}} \quad \forall t \in \mathcal{T}, \forall i \in \mathcal{H}^H \quad (6e)$$

Finally, the total energy cost of a single HHP across the optimization horizon can be computed as:

$$J_{i,t}^c = \lambda_t^c \cdot P_{i,t}^{\text{HP}} \cdot \Delta t + \lambda^g \cdot g^t \quad \forall t \in \mathcal{T}, \forall i \in \mathcal{H}^H \quad (7a)$$

$$(1/\Delta t) \cdot g_{i,t} \eta^g H^g = \Phi_{i,t}^{\text{CV}} \quad \forall t \in \mathcal{T}, \forall i \in \mathcal{H}^H \quad (7b)$$

C. Thermal Comfort Quantification

The Predicted Mean Vote (PMV) and the Predicted Percentage of Dissatisfied (PPD) are widely used to assess thermal

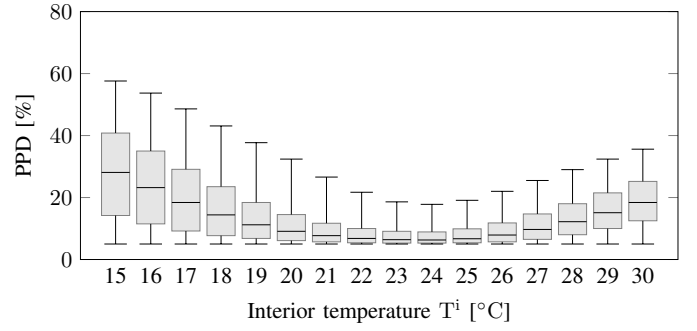


Fig. 2. Distribution of PPD for $T_i \in [15, 30]$ °C as derived from kernel density estimation.

comfort performance [15]. The PMV is derived by expanding the comfort equation based on the seven-point ASHRAE thermal sensation scale, which ranges from -3 (cold) to $+3$ (hot), with intermediate values representing varying levels of thermal comfort: -2 (cool), -1 (slightly cool), 0 (neutral), $+1$ (slightly warm), and $+2$ (warm). PPD tells how many people may feel uncomfortable. If PPD is high, many people are too hot or too cold. A low PPD means most people feel comfortable.

It is important to note that the PMV and PPD equation is quite complex, and its detailed formulation can be found in the relevant literature [24]. Therefore, we did not calculate PMV directly. Instead, we utilized data from the ASHRAE Global Database II [25], which includes information on factors such as clothing insulation, metabolic rate, and other relevant variables. We selected over ten thousand measurements collected from temperate regions of Europe. Kernel Density Estimation (KDE) was employed to estimate the probability density function (PDF) of the radiant temperature, air velocity, relative humidity, clothing insulation, and metabolic rate. For a combination of factors, the PPD was calculated using the Python package *pythermalcomfort* [26]. Through repeated random sampling, ranges of PPD for a given indoor temperature were calculated, as shown in Fig. 2.

After that, we proceed with the linearization of PPD for integration into the overall optimization objective. Since the set of PPD points within the given interior temperature range $T_i \in [15, 30]$ °C is approximately quadratic and hence convex we can use an outer approximation to find an equivalent linear formulation. The outer approximation can be defined as:

$$\text{PPD}_{i,t} \geq f(T_{i,t}, \mu_m, \mu_{m+1}) \quad \forall t \in \mathcal{T}, \forall i \in \mathcal{H}_{\text{HP}}, \forall m \in \mathcal{M} \quad (8)$$

Where $f(T_{i,t}, \mu_m, \mu_{m+1})$ is the line $f(T_{i,t}^i)$ passing through the two median points $\{\mu_m, \mu_{m+1}\} \subset \mathcal{M}$ with \mathcal{M} the set of median PPD points described by Fig. 2. The outer approximation is visualized in Fig. 3.

D. Congestion Management Model

For the entire model, the optimization objective combines the total energy cost and the comfort cost. By integrating the network model, thermal dynamics model, and HHPs, we propose the complete optimization model, as shown in (9).

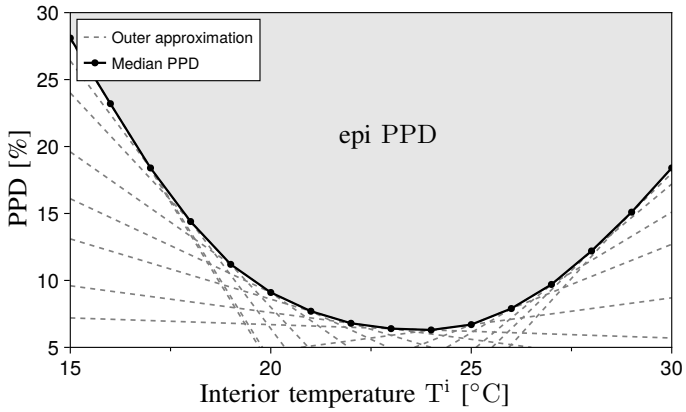


Fig. 3. Outer approximation of the PPD objective.

$$\begin{aligned}
 \min \quad & \sum_{\mathcal{T}} \lambda_t^p \Delta t \left(\sum_{\mathcal{H}} p_{i,t} + \sum_{(i,j) \in \mathcal{L}} r_{i,j} l_{i,j} \right) + \sum_{\mathcal{T}} \lambda_t^g g_{i,t} \\
 & + \underbrace{\sum_{\mathcal{T}} \lambda_{\text{comf}} \cdot \text{PPD}_{i,t}}_{\text{Comfort Cost}} \\
 \text{s.t.} \quad & \text{Network model: (Eqs. (1)-(3))} \\
 & \text{Thermal dynamics: (Eq. (4))} \\
 & \text{HHP model: (Eqs. (5)-(7))}
 \end{aligned} \tag{9}$$

To optimize congestion management, a baseline case is first established based on the historical data from the project without implementing any specific congestion measures. This baseline result p_t^{baseline} serves as a reference for comparing and quantifying the impact of the measures applied subsequently. We regulate the imported power to follow the power reduction request p_t^{flex} specified for the selected time period $\mathcal{T}_{\text{congestion}}$. The total imported power should obey the set power limit during congestion management as enforced by (10).

$$p_t^{\text{imp}} \leq p_t^{\text{baseline}} - p_t^{\text{flex}} \quad \forall t \in \mathcal{T}_{\text{congestion}} \tag{10}$$

III. CASE STUDY

A. Case Description

This study selects a section of a real low-voltage distribution network in the Netherlands. The network data are extracted from the network information file, as illustrated in Fig. 4. The system comprises 87 nodes, including 37 residential load nodes, 12 of which are equipped with HHPs. The thermal properties of the houses and the operational parameters of the HHPs are assumed to be identical for all customers. For the thermal comfort price, we keep the λ_{comf} constant and equal to 0.27 €/‰ [15]. We collected energy consumption data from real users on one day (February 1, 2024) as the test case. After simulating the power flow operation based on the real case, we presented the voltage deviation of each node in Fig. 4. Since this case only considers the consumers' load, the voltage at the nodes is always lower than that of the slack bus. Some

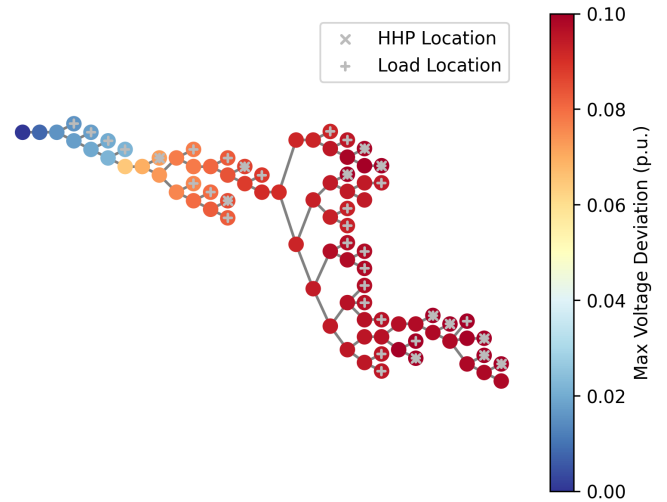


Fig. 4. Low-voltage distribution network topology: Node voltage deviation from the slack.

of the voltage deviations came close to 0.1 p.u., which is the maximum allowable deviation set in this low-voltage system.

For this study, we focus on the selected day during the peak hours from 17:00 to 19:00, when congestion management is required by the DSO. To analyze the impact of power limitations, we evaluate three power limitation scenarios: 4 kW, 8 kW, and 12 kW.

B. Result and Analysis

The costs associated with different congestion management cases are analyzed in Table II. The flexibility price is defined as the total additional cost divided by the flexibility provided. As the power limitation increases, the flexibility price remains approximately 0.3 €/kWh, but the marginal increase in provided flexibility gradually declines.

Specifically, in the 4 kW limit case, the additional comfort cost is almost twice the total additional cost, which indicates that the system consumes less energy and tolerates a higher comfort cost. Whereas with a higher limit, addition comfort cost increases less, but total additional cost increases more, which finally makes two costs almost the same in the 12kW case. This indicates that the system consumes more energy to maintain an acceptable level of comfort with higher power limitation.

The total power in four different limit scenarios is shown in Fig. 5, where the basic load represents the consumers' load without the HHP, obtained from historical data. During the period from 17:00 to 19:00 (the gray area in the figure), the aggregated peak power is regulated to comply with the power limit requirements. By utilizing the flexibility of the HHPs, the system changes the HP load to reduce the total load. Meanwhile, before the congestion period, the HHPs operate at higher output levels, and then their load decreases sharply during the power limitation period.

For detailed user information, Fig. 6 illustrates the indoor temperatures of all 37 residents across different power limit

TABLE II
ANALYSIS OF DIFFERENT POWER LIMITATIONS

| | 4 kW | 8 kW | 12 kW |
|------------------------------------|------|-------|-------|
| Total Additional Cost (€) | 1.73 | 2.81 | 4.34 |
| Additional Comfort Cost (€) | 3.41 | 3.87 | 4.91 |
| Flexibility Provided (kWh) | 6.77 | 10.34 | 12.43 |
| Flexibility Price (€/kWh) | 0.26 | 0.27 | 0.35 |

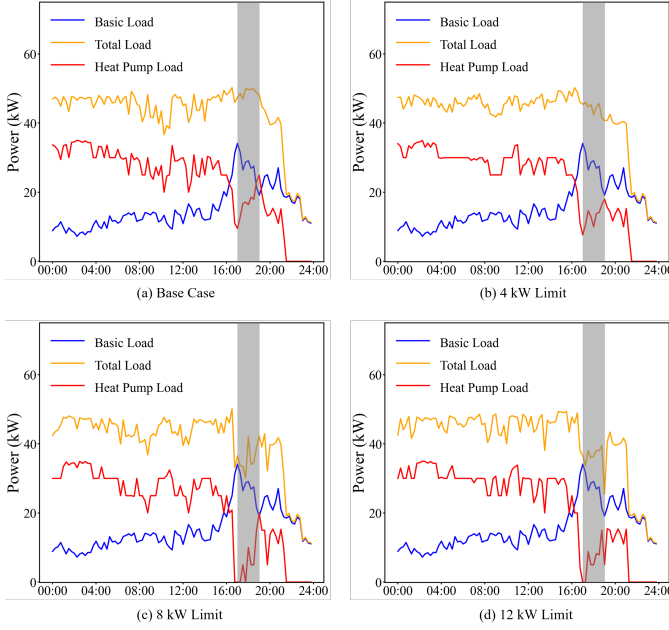


Fig. 5. Load in base case and different power limit cases with the regulated period in the gray.

cases. The actual outdoor temperature is measured by the smart meters within DACS. As figure shows, the outdoor temperature is lower during the congestion period than in the afternoon, so the indoor temperature is more likely to decrease, as modeled in Eq. 4a. To address this issue, indoor temperatures are preheated for different users before the congestion period.

Notably, temperatures in the base case would not exceed 23°C , which represents the optimal comfort point as shown in Fig. 2, whereas in power limitation cases, the temperature for some users would exceed 23°C . For this, Fig. 7 provides the information about the PPD of all users in each case. During the power limitation period, the PPD of users with a temperature higher than 23°C tends to remain stable.

During the whole congestion management process, different users exhibit distinct temperatures, with varied HP usage allocations during flexibility provision, as shown in Fig. 8. Although most parameters are set consistently, differences in inherent load profiles and network topology lead to variations in power and voltage constraints. As a result, users require different HP allocations to achieve optimal results of both energy consumption and comfort levels.

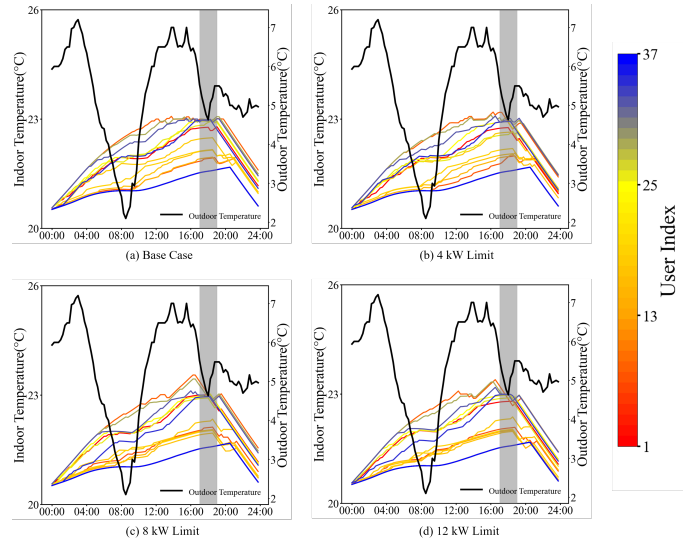


Fig. 6. Indoor temperature and outdoor temperature in different scenarios with the regulated period in the gray.

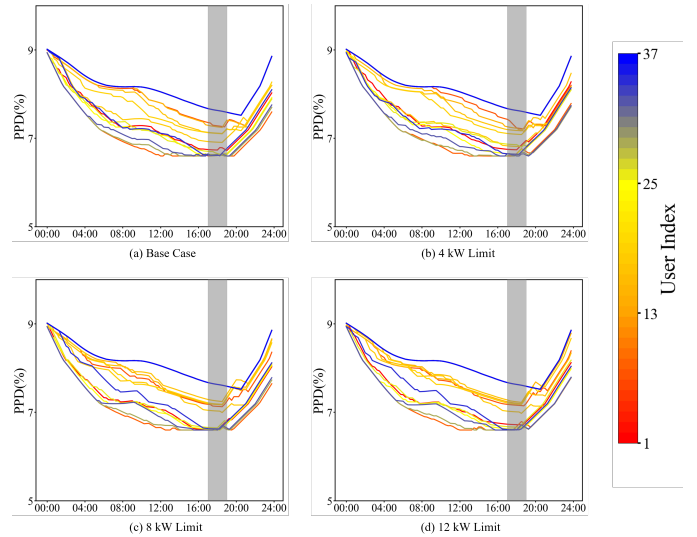


Fig. 7. PPD of all users in base case and different power limit cases with the regulated period in the gray.

IV. CONCLUSION

This paper presents a quantified thermal comfort model in congestion management to allocate flexibility among HHPs during power limitation periods. By including thermal comfort in the optimization objective, the user comfort cost during congestion management is optimized together with energy cost. Under different levels of power limitation, the corresponding flexibility allocation and thermal comfort among users vary even when the same technical parameters are applied. This variation may lead to potential fairness issues among users in real congestion management scenarios. Our study also shows that different power limits can result in varying flexibility prices. However, the price simulated here is based on the comfort price we set, which could be further investigated based

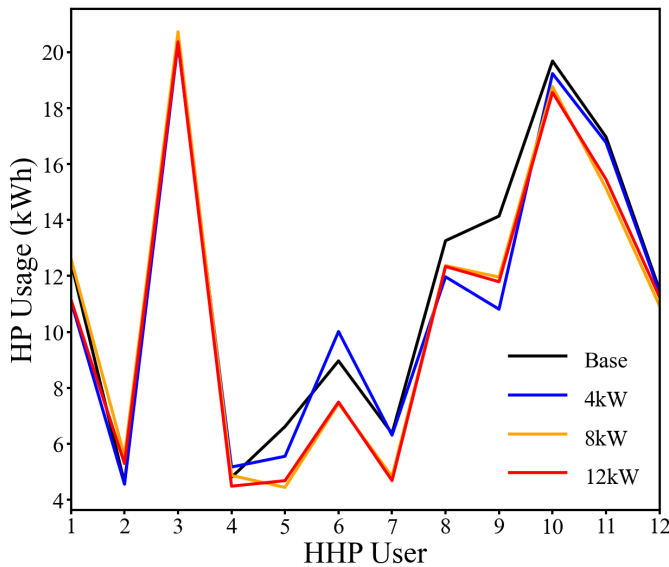


Fig. 8. HP usage of different HHP users.

on real users' preferences.

REFERENCES

- [1] Grid congestion gets companies negotiating with grid operators. [Online]. Available: <https://www.abnamro.com/en/news/grid-congestion-n-gets-companies-negotiating-with-grid-operators>
- [2] T. Vo, A. Haque, P. Nguyen, I. Kamphuis, M. Eijgelaar, and I. Bouwman, "A study of congestion management in smart distribution networks based on demand flexibility," in *2017 IEEE Manchester PowerTech*. IEEE, 2017, pp. 1–6.
- [3] TenneT. Congestion management for off-take and feed-in. [Online]. Available: <https://www.tennet.eu/markets/dutch-market/congestion-management-take-and-feed>
- [4] Netherlands Enterprise Agency, RVO. Hybrid heat pumps become mandatory when replacing boiler. [Online]. Available: <https://business.gov.nl/amendment/hybrid-heat-pump-mandatory/>
- [5] P. Fitzpatrick, F. D'Ettoire, M. De Rosa, M. Yadack, U. Eicker, and D. P. Finn, "Influence of electricity prices on energy flexibility of integrated hybrid heat pump and thermal storage systems in a residential building," *Energy and Buildings*, vol. 223, p. 110142, 2020.
- [6] E. Carter, O. Lancaster, and F. Chanda, "Early results from the freedom project: fully-optimised hybrid heat pumps providing demand flexibility," in *12th IEA heat pump conference 2017: Rotterdam*, 2017.
- [7] K. J. Chua, S. K. Chou, and W. Yang, "Advances in heat pump systems: A review," *Applied energy*, vol. 87, no. 12, pp. 3611–3624, 2010.
- [8] R. D'hulst, W. Labeeuw, B. Beusen, S. Claessens, G. Deconinck, and K. Vanthournout, "Demand response flexibility and flexibility potential of residential smart appliances: Experiences from large pilot test in Belgium," *Applied Energy*, vol. 155, pp. 79–90, 2015.
- [9] H. Li, Z. Wang, T. Hong, and M. A. Piette, "Energy flexibility of residential buildings: A systematic review of characterization and quantification methods and applications," *Advances in Applied Energy*, vol. 3, p. 100054, 2021.

- [10] G. Reynders, R. A. Lopes, A. Marszal-Pomianowska, D. Aelenei, J. Martins, and D. Saelens, "Energy flexible buildings: An evaluation of definitions and quantification methodologies applied to thermal storage," *Energy and Buildings*, vol. 166, pp. 372–390, 2018.
- [11] W. O'Brien, I. Gaetani, S. Carlucci, P.-J. Hoes, and J. L. Hensen, "On occupant-centric building performance metrics," *Building and Environment*, vol. 122, pp. 373–385, 2017.
- [12] S. Zhan, T. Gu, W. van den Akker, W. Brus, A. van der Molen, and J. Morren, "Towards congestion management in distribution networks: a dutch case study on increasing heat pump hosting capacity," in *12th IET International Conference on Advances in Power System Control, Operation and Management (APSCOM 2022)*, vol. 2022, 2022, pp. 364–369.
- [13] J. Fang, Z. Feng, S.-J. Cao, and Y. Deng, "The impact of ventilation parameters on thermal comfort and energy-efficient control of the ground-source heat pump system," *Energy and Buildings*, vol. 179, pp. 324–332, 2018.
- [14] F. Pallonetto, M. De Rosa, and D. P. Finn, "Impact of intelligent control algorithms on demand response flexibility and thermal comfort in a smart grid ready residential building," *Smart Energy*, vol. 2, p. 100017, 2021.
- [15] X. Xu, W. Hu, W. Liu, Y. Du, R. Huang, Q. Huang, and Z. Chen, "Risk management strategy for a renewable power supply system in commercial buildings considering thermal comfort and stochastic electric vehicle behaviors," *Energy Conversion and Management*, vol. 230, p. 113831, 2021.
- [16] L. Jin, X. Li, S. De Lange, H. Slootweg, and N. G. Paterakis, "Response allocation of domestic hybrid heat pumps flexibility for congestion management," in *2024 IEEE PES Innovative Smart Grid Technologies Europe (ISGT EUROPE)*, 2024, pp. 1–5.
- [17] Digitale aggregatie en collectieve sturing van hybride warmtepompen (dacs-hw). [Online]. Available: <https://dacs-hw.nl/>
- [18] M. M.-U.-T. Chowdhury, S. Kamalasadana, and S. Paudyal, "A second-order cone programming (socp) based optimal power flow (opf) model with cyclic constraints for power transmission systems," *IEEE Transactions on Power Systems*, vol. 39, no. 1, pp. 1032–1043, 2024.
- [19] M. Farivar and S. H. Low, "Branch flow model: Relaxations and convexification—part i," *IEEE Transactions on Power Systems*, vol. 28, no. 3, pp. 2554–2564, 2013.
- [20] P. Bacher and H. Madsen, "Identifying suitable models for the heat dynamics of buildings," *Energy and Buildings*, vol. 43, no. 7, pp. 1511–1522, 2011.
- [21] G. Verhoeven, B. Van der Holst, and S. C. Doumen, "Modeling a domestic all-electric air-water heat-pump system for discrete-time simulations," in *2022 57th International Universities Power Engineering Conference (UPEC)*, 2022, pp. 1–6.
- [22] B. van der Holst, G. Verhoeven, P. Nguyen, K. Kok, M. Emde, J. Nutma, and S. la Fleur, "A Quantification Method for the Potential Downward Flexibility of Full-Electric Heat Pumps during Congestion Events," in *2023 IEEE Belgrade PowerTech*. IEEE, 2023, pp. 01–06.
- [23] C. Verhelst, D. Degrauwe, F. Logist, J. Van Impe, and L. Helsen, "Multi-Objective Optimal Control of an Air-to-Water Heat Pump for Residential Heating," in *Building Simulation*, vol. 5. Springer, 2012, pp. 281–291.
- [24] P. Fanger, "Thermal comfort: Analysis and applications in environmental engineering," 1970.
- [25] ASHRAE global database of thermal comfort field measurements. [Online]. Available: <https://datadryad.org/stash/dataset/doi:10.6078/D1F671>
- [26] F. Tartarini and S. Schiavon, "pythermalcomfort: A python package for thermal comfort research," *SoftwareX*, vol. 12, p. 100578, 2020.